

3D Casing-Source Electromagnetic Modeling for CO₂ Plumes and Enhanced Geothermal Systems Monitoring

Evan Schankee Um and David L. Alumbaugh
Earth and Environmental Sciences, Lawrence Berkeley National Laboratory, Berkeley, CA, USA

SUMMARY

We present a modeling workflow that combines 3D cylindrical-mesh-based and rectangular-mesh-based electromagnetic (EM) modeling codes for efficiently simulating EM responses where steel well casings are employed as part of a grounded electrical source. Our modeling examples include 3D casing source scenarios with a single vertical well, multiple vertical wells, and a deviated steel-cased well. The workflow that is described involves approximating the energized casing with a series of electric dipoles, and has been employed to determine the sensitivity of different EM data acquisition scenarios for monitoring in complex 3D environments such as CO₂ storage and engineered geothermal system (EGS) sites.

Keywords: EM Casing Source, 3D numerical modeling, monitoring, CO₂, and geothermal

INTRODUCTION

Incorporating highly-conductive steel-cased wells into electromagnetic (EM) earth models is motivated by the possibility of utilizing long metal-cased wells as enhanced EM sources. This casing source can amplify source dipole moments and enable greater signal penetration at depth for monitoring subsurface processes (Schenkel and Morrison, 1990; Daily et al., 2004; Marsla et al., 2014; Commer et al., 2015). This enhancement allows us to detect and image deep-localized targets that traditional surface EM survey configurations may not be sensitive enough to identify. Recently, these casing source EM methods have been applied to a range of geophysical problems, including CO₂ monitoring (e.g., MacLennan et al., 2016; Puzyrev et al., 2017), fracture imaging (Weiss et al., 2016; Li and Yang, 2019; Um et al., 2019), enhanced geothermal system monitoring (e.g., Castillo-Reyes et al., 2021; Alumbaugh et al., 2023).

Simulating a hollow casing string in a 3D reservoir-scale or regional-scale EM earth model poses numerical challenges. For example, discretizing a casing in the 3D rectangular coordinate system requires a large number of fine cells due to the thinness of a casing. The exponential increase in required cells with well length makes 3D modeling using true casing geometry less practical in the 3D rectangular coordinate system, even on a parallel computer (e.g., Commer et al., 2015). While 3D cylindrical-mesh-based EM modeling codes (e.g., Heagy and Oldenburg, 2022) excel at accurately discretizing a hollow vertical cased well with a relatively small number of cells, challenges arise in dealing with complex 3D background models or deviated wells that no longer align with the cylindrical coordinate system. Alternatively, Weiss et al (2017) and Li and Yang (2019) use a hierarchical earth model and an equivalent resistor network, respectively to economically represent cased wells. Um et al. (2020) approximate cased wells using a volumeless boundary condition.

This paper presents a 3D EM modelling workflow designed for simulating a 3D casing source EM model having complex background resistivity structures at reduced computational costs compared to explicit casing discretization in the rectangular coordinate system. Rather than developing a new modelling algorithm for casing source EM simulations, we take a synergistic approach by utilizing two existing 3D EM modelling codes: the 3D SimPEG code (Heagy and Oldenburg, 2022) and the 3D finite-element EM code (Um et al., 2020). By integrating the strengths of each code, we leverage their advantages to address challenges in casing EM modelling. Following the demonstration of the workflow concept, we explore its applicability and limitations in dealing with deviated wells and multiple well scenarios.

WORKFLOW FOR SIMULATING EM CASING SOURCE

We first describe a modelling workflow that approximates the EM effects of an energized steel-cased well in a vertical orientation. Subsequently, we explore the applicability and limitations of this workflow in the context of deviated well and multiple well scenarios.

The workflow comprises five steps. First, we create a layered earth model with resistivity structure aligned with that along the path of a vertical well (step 1). This step requires a 3D resistivity model of the area or at least resistivity logging data. Next, we employ the 3D SimPEG code (Heagy and Oldenburg, 2022) to simulate energizing the vertical well. This simulation, fitting naturally within the cylindrical coordinate system, typically completes in less than an hour on a PC. Following the simulation, we extract the vertical electric current density along the outer surface of the well (step 3). The resulting set of equivalent dipoles is then mapped along the well trajectory in the 3D earth model (step 4), which is discretized using

unstructured tetrahedral meshes. Unlike cylindrical meshes, tetrahedral meshes are well suited for discretizing complex geology structures. Last, the resulting 3D model is simulated using the 3D finite-element modelling code (Um et al., 2020).

In the numerical modeling examples presented in this paper, we assume a consistent single casing thickness throughout the well and a uniform current density across the casing's cross-sectional area at each depth. This allows us to simply calculate the total casing current by multiplying the well's cross-sectional area by the current density on its outer surface. However, note that this assumption may not hold when casings are nested, resulting in variations in current distribution across the cross-section. In such cases, modeling the nested well structures is required, and the casing current is computed by integrating the current density over the entire cross-sectional area. While this modeling scenario is more involved, it can still be effectively modeled using the 3D SimPEG code. In short, the workflow is applicable to models that involve both 3D complex background and nested cased well.

3D CASING SOURCE EM MODELING EXAMPLES

1. Single Vertical Steel-Cased Well

First, the workflow is demonstrated with a straightforward example involving a single vertical well energized by a top-casing source configuration. In this example, a steel-cased well is 1 km deep, and the source electrode is connected to the top of the well casing (electrical conductivity: 10^6 S/m; outer radius: 0.1 m; thickness: 0.02 m). The return surface electrode is grounded 2 km away from the well head.

The source frequency is set to 1 Hz. The earth resistivity model is set to a 100 Ohm-m homogeneous half-space. A vertical observation well is situated 500 m away from the source well and vertical electric fields are measured there.

This vertical well problem can be efficiently simulated using the 3D SimPEG code without any additional steps. We first simulate this top-casing source configuration and next extract a set of casing current densities along the source well and vertical electric fields along the observation well. For evaluation, the extracted casing currents are compared against a Method of Moments (MoM) solution (Tang et al., 2015), and this comparison provides good agreement between the two solutions (**Figure 1a**). Subsequently, the extracted casing densities replace the energized steel-cased well in a 3D finite element EM model. The resulting finite element solution at the observation well is compared to the 3D SimPEG solution, again demonstrating good agreement (**Figure 1b**).

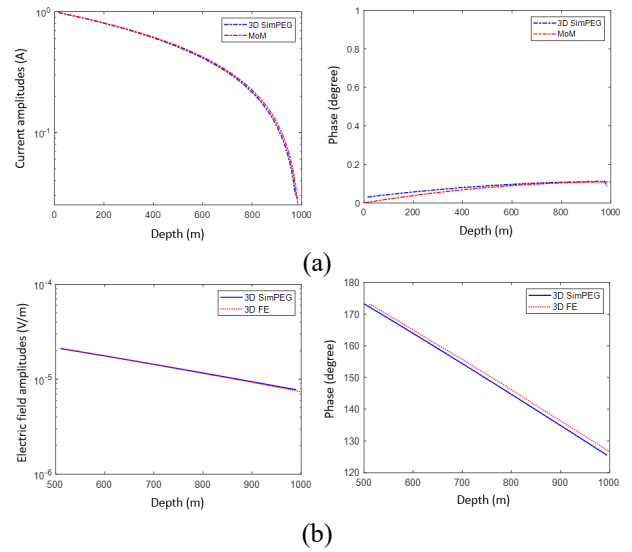


Figure 1. (a) Comparisons between the current density amplitudes calculated using the 3D SimPEG and MoM method. (b) Comparisons between borehole vertical electric field amplitudes calculated using true casing geometry (SimPEG) and equivalent sources (3D FE solutions).

2. Simulating a Multiple Vertical Casing Source EM at a proposed CO₂ Storage Site

Next, we explore the potential of the casing-source EM method for CO₂ sequestration monitoring at the Wyoming CarbonSAFE project (**Figure 2**) adjacent to the Dry Fork Station coal fired power plant in Gillette, Wyoming (Sullivan et al., 2020).

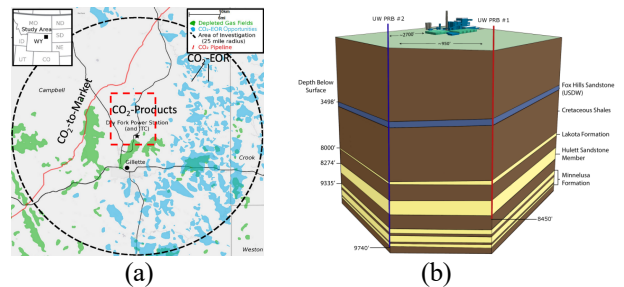


Figure 2. (a) Map showing the location of Dry Fork Station (b) Dry Fork Station Integrated Test Centre (Source: <https://www.uwyo.edu/cegr/research-projects/wyoming-carbonsafe.html>)

Figure 3a shows the layered resistivity model at the CO₂ storage site estimated from the well logging data and geological information. The layering becomes more detailed in the vicinity of the five proposed injection zones, indicated as indicated in the Table in **Figure 3a** as **. We apply Archie's Law to estimate resistivities for the five injection zones during and after CO₂ injection assuming a CO₂ saturation of 60%. The resulting

resistivity values for the five injections zones are shown in the table below.

	Porosity	Reservoir Resistivity (Sw=1)	Fluid Resistivity	Reservoir Resistivity (Sw=0.4, Sco2=0.6)
Reservoir 1	0.35	3	0.61	30.93
Reservoir 2	0.3	2	0.42	29.46
Reservoir 3	0.2	3	0.35	54.13
Reservoir 4	0.15	4	0.30	83.33
Reservoir 5	0.1	6	0.24	153.09

For numerical purposes, we implement an upscaling procedure for the zones within and between the intended thin injection zones, creating thicker reservoir injection units. Specifically, we consider a 90m thick zone spanning from 2455 to 2545 m depth to represent the upper injection zone in one injection well (PRB1). Additionally, we include a 60m thick zone ranging from 2851 m to 2910 m to cover the planned lower injection intervals in the other injection well (PRB2). This upscaling is necessary to avoid the inclusion of excessively thin and elongated cells within the numerical model which makes the finite element solution numerically costly and less efficient.

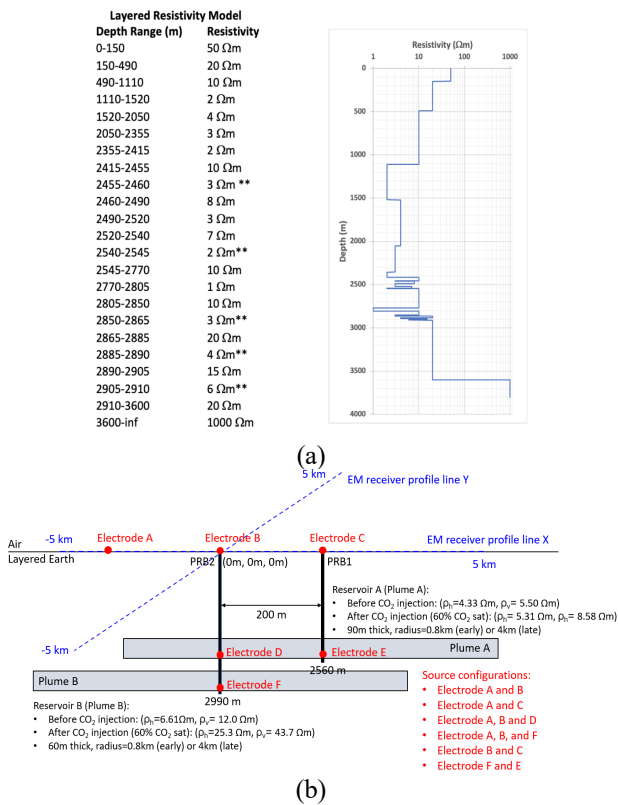


Figure 3. (a) The 1D resistivity model at the Wyoming CarbonSAFE site. (b) The 3D resistivity models used for the Wyoming CarbonSAFE site. The background layered resistivity model outside of the injection zones is described by the thicker layers in Figure 3a. The thinner layers within injection zones have been upscaled to Plume A and B as shown here.

To account for the current flow within the alternating conductive and resistive layers for the models that include the thin layers of injected CO₂, we calculated resistivities within these zones using an anisotropic approach. We determined the vertical resistivity (ρ_v) as the geometric mean of the layer resistivities and the horizontal resistivity (ρ_h) as the harmonic mean. This calculation results in injection zones depicted in Figure 3 that exhibit lower resistivity in the horizontal direction compared to the vertical direction, mimicking current flow patterns similar to alternating conductors and resistors. Employing these upscaled resistivity values, we created two distinct plume models, as illustrated in Figure 3b: an 'early' plume representing a relatively short time after injection initiation and a 'late' plume simulating conditions akin to 20 years of injection.

Various casing source configurations were tested, as listed in Figure 3b. In this study, we highlight a casing source configuration where one electrode is connected to the bottom of PRB2, and the other is connected to the bottom of PRB1. To simulate this setup, we calculate the current densities along PRB2 with one electrode connected to its bottom (electrode F) and the other grounded to the surface (electrode A). Similarly, we repeat the calculation for current densities along PRB1 using electrodes A and E. Note that the opposite current direction is used in the latter case. By superposing these two sets of current densities, we approximate the casing current distribution along the two wells energized by the two bottom electrodes. Note that this is an approximation as any EM interaction between the two cased wells is ignored. At the frequency used here (0.25 Hz) the skin depth within the steel casing assuming a relative magnetic permeability of 100 and an electrical conductivity of 10⁶ S/m is approximately 0.10m which is much thicker than the casing itself. Thus, we infer that any EM mutual inductive effects are negligible compared to normal galvanic current leakage, and thus the combined-casing source response can be treated as a summation of the two individual responses. Figure 4 shows that the proposed casing source EM layout can produce measurable perturbations as a result of CO₂ injection over time.

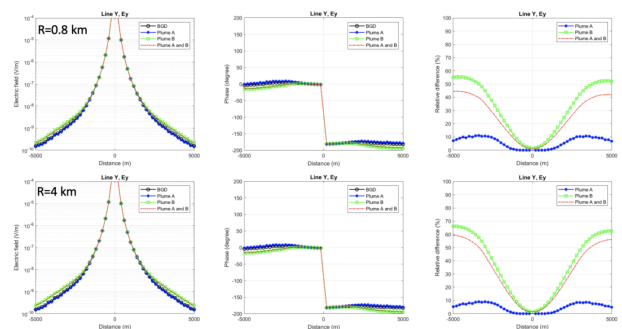


Figure 4. Ey components at 0.25Hz along line Y (Figure 3b) for the source connecting points E and F.

3. Deviated Casing Source EM at Utah FORGE site

In the last example we consider energizing a deviated steel-cased well, which is used as an injection well at the Utah FORGE EGS test site (Moore et al., 2019). Our focus is to assess whether casing source EM responses are sensitive to the stimulated zone at the FORGE site. **Figure 5** shows the locations of the injection well (16-78(32)) as well as the 3D electrical resistivity model which is based on 3D MT inversion (Wannamaker et al., 2020). The size and electrical resistivity of the stimulated zone are based on Discrete Fracture Network modeling analysis (Finnila and Podgorny, 2020). We examine two fracture models. Fracture model 1 has resistivities of 2970 Ωm in the x -axis and 190 Ωm in the y - and z -axes. Fracture model 2 features resistivities of 302 Ωm , 270 Ωm , and 256 Ωm in the x -, y -, and z -axes, respectively. The downhole electrode is positioned at a depth of 1 km in the injection well, while the surface electrode is grounded 1.4 km away from the wellhead. The casing source EM responses are measured in observation wells 58-32 and 78B-32 using a three component high temperature EM sensor called the vertical EM profiling system (VEMP) (Wilt et al., 1997)

To apply the workflow to the deviated well, we construct a layered resistivity model aligning with the resistivity structure along the trajectory of the deviated injection well (16A-78(32)) in the 3D FORGE MT model (**Figure 5b**). Next, a vertical steel-cased well whose depth is the same as the measured length of the deviated well is inserted into the layered model. Finally, using the 3D SimPEG code, we simulate energizing the vertical well. The casing current densities are extracted along the vertical well from the SimPEG model and distributed along the actual trajectory of the deviated well in the 3D earth model. Note that the effects of casing's magnetic permeability are not considered here.

An important question is whether the casing current distribution from the verticalized steel-cased well can reasonably represent that of the true deviated well. In general, the current distribution from a verticalized well may not always closely resemble its deviated counterpart, because of the differing impact of a surface-grounded return electrode. In the context of the FORGE site, however, the proposed workflow is expected to be effective due to several key factors: 1) a highly-conductive steel-cased well is embedded in highly-resistive granite bedrock within the zone where measurements will be made, 2) the shallow area where the well is vertical is covered with conductive sediments, 3) the downhole electrode is positioned at a substantial depth (i.e., 1 km) beneath the surface, and 4) a return electrode on the surface is grounded sufficiently distant (i.e., 1.4 km) from the well. Hence, at the FORGE site, the primary factor influencing casing current distribution and the rate at which the current 'leaks' into the formation is reasonably assumed to be the

resistivity contrast between the casing and the background resistivity, rather than the position of the return electrode or other factors. Thus, it is logically inferred that the current distribution along the vertical well reasonably represents the distribution for the deviated well. **Figure 6** shows casing source EM responses with and without fractures, indicating measurable signal amplitudes and sensitivity to both fracture models.

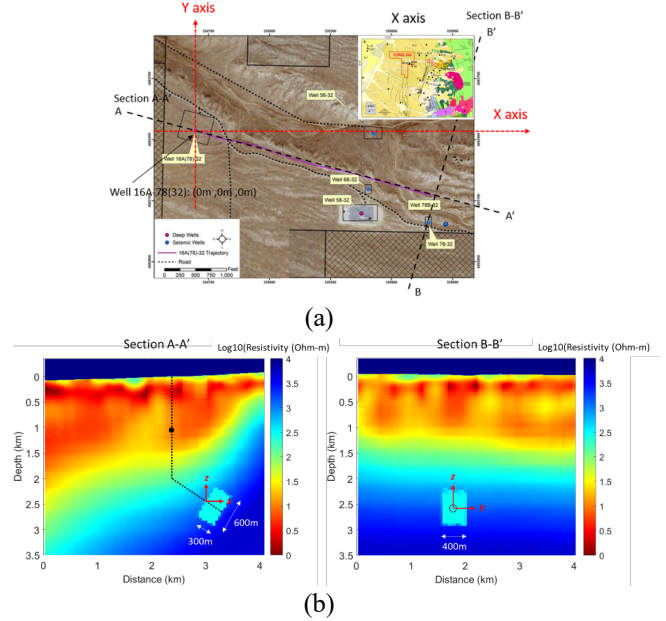


Figure 5. (a) The Utah FORGE map showing the injection well and other observation wells. The red broken lines indicate a coordinate system with the center set at the wellhead of the injection well. The trajectory of the deviated part of the injection well is indicated by the magenta line. (b) A-A' (left) and B-B' (right) cross-sections of the Utah FORGE MT model featuring an expected stimulated fracture zone and a local coordinate system (red) used for describing the orientation of the fracture system.

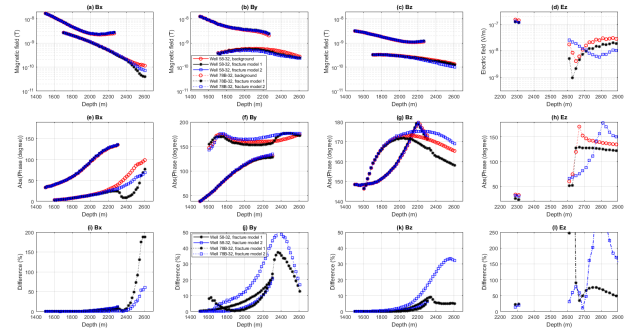


Figure 6. Comparison in EM measurements (the 1st row) at 50 Hz before and after stimulation, the phase (the 2nd row) and their relative amplitude differences (the 3rd row). The surface electrode is grounded at (-1.4km, 0km, 0km).

CONCLUSION

We have introduced a novel modeling workflow designed for the efficient simulation of casing source EM responses in a 3D complex geology model. This approach combines the strengths of both 3D cylindrical-mesh-based and 3D tetrahedral-mesh-based EM modeling codes. Through illustrative examples, we have demonstrated the effectiveness of our workflow in scenarios involving a vertical cased well, multiple vertical cased wells, and a single deviated cased well. While we acknowledge that our proposed workflow may not encompass all the details associated with casing EM modeling, we believe it can serve as a valuable first-order approximation for assessing casing source EM responses to realistic 3D geology model.

ACKNOWLEDGMENTS

This research received support from the Utah FORGE project and DOE's Core Carbon Storage and Monitoring Research program, sponsored by the U.S. Department of Energy under Contract No. DE-AC02-05CH11231.

REFERENCES

- Alumbaugh, D., Um, E., Wilt, W., Nichols, E., and Osato, K. 2023. Deep Borehole EM Deployment for Fracture Mapping at the FORGE Geothermal Site. In Proceedings of the 48th Workshop on Geothermal Reservoir Engineering, Stanford, California.
- Castillo-Reyes, O., Queralt, P., Marcuello, A., & Ledo, J. (2021). Land CSEM simulations and experimental test using metallic casing in a geothermal exploration context: Vallès basin (NE Spain) case study. *IEEE Transactions on Geoscience and Remote Sensing*, 60, 1-13.
- Commer, M., Hoversten, G.M. and Um, E.S., 2015. Transient-electromagnetic finite-difference time-domain earth modeling over steel infrastructure. *Geophysics*, 80(2), E147-E162.
- Daily, W., Ramirez, A., Newmark, R. and Masica, K., 2004. Low-cost reservoir tomographs of electrical resistivity. *The Leading Edge*, 23(5), 472-480.
- Finnila, A., and Podgorney, R. 2020. Exploring hydraulic fracture stimulation patterns in the forge reservoir using multiple stochastic DFN realizations and variable stress conditions. In Proceedings of the 45th Workshop on Geothermal Reservoir Engineering.
- Heagy, L.J. and Oldenburg, D.W., 2022. Electrical and electromagnetic responses over steel-cased wells. *The Leading Edge*, 41(2), 83-92.
- Hu, Y., Yang, D., Li, Y., Wang, Z. and Lu, Y., 2021. 3-D numerical study on controlled source electromagnetic monitoring of hydraulic fracturing fluid with the effect of steel-cased wells. *IEEE Transactions on Geoscience and Remote Sensing*, 60, 1-10.
- Lee, K.H., Kim, H.J. and Uchida, T., 2005. Electromagnetic fields in a steel-cased borehole. *Geophysical prospecting*, 53(1), 13-21.
- Li, Y. and Yang, D., 2019. Fast electrical imaging of injected fluid in hydraulic fracturing using a practical interactive parameter estimation method. In SEG Technical Program Expanded Abstracts 2019, 1024-1028, Society of Exploration Geophysicists.
- Marsala, A.F., Hibbs, A.D. and Morrison, H.F., 2014, October. Borehole casing sources for electromagnetic imaging of deep formations. In SPE Annual Technical Conference and Exhibition? (SPE-170845). SPE.
- MacLennan, K., Nieuwenhuis, G., Ramadoss, V., Wilkinson, M., Anderson, P., and Richards, T., 2016, October. Using depth to surface resistivity for mapping CO₂. In 2016 SEG International Exposition and Annual Meeting.
- Puzyrev, V., Vilamajo, E., Queralt, P., Ledo, J. and Marcuello, A., 2017. Three-dimensional modeling of the casing effect in onshore controlled-source electromagnetic surveys. *Surveys in Geophysics*, 38, 527-545.
- Schenkel, C.J. and Morrison, H.F., 1990, Effects of well casing on potential field measurements using downhole current sources, *Geophysical Prospecting*, 38(6), 663-686.
- Sullivan, M., Rodosta, T., Mahajan, K. and Damiani, D., 2020. An overview of the Department of Energy's CarbonSAFE Initiative: Moving CCUS toward commercialization. *AIChE Journal*, 66(4), e16855.
- Tang, W., Li, Y., Swidinsky, A., and Liu, J. 2015. Three-dimensional controlled-source electromagnetic modelling with a well casing as a grounded source: a hybrid method of moments and finite element scheme. *Geophysical Prospecting*, 63, 1491-1507.
- Um, E.S., Kim, J., Wilt, M.J., Commer, M. and Kim, S.S., 2019. Finite-element analysis of top-casing electric source method for imaging hydraulically active fracture zones. *Geophysics*, 84(1), E23-E35.

Um, E.S., Kim, J. and Wilt, M., 2020. 3D borehole-to-surface and surface electromagnetic modeling and inversion in the presence of steel infrastructure. *Geophysics*, 85(5), E139-E152.

Wannamaker, P., Simmons, S., Miller, J., Hardwick, C., Erickson, B., Bowman, S., Kirby, S., Feigl, K., and Moore, J. 2020. Geophysical Activities over the Utah FORGE Site at the Outset of Project Phase 3. Proceedings, 45th Workshop on Geothermal Reservoir Engineering, Stanford University, Stanford, CA.

Weiss, C.J., Aldridge, D.F., Knox, H.A., Schramm, K.A. and Bartel, L.C., 2016. The direct-current response of electrically conducting fractures excited by a grounded current source. *Geophysics*, 81(3), E201-E210.

Weiss, C.J., 2017. Finite-element analysis for model parameters distributed on a hierarchy of geometric simplices. *Geophysics*, 82(4), E155-E167.

Wilt, M., Takasugi, S., Uchida, T., Kasameyer, P., Lee, K. and Lippmann, M. 1997. Fracture mapping in geothermal fields with long-offset induction logging. In Proceedings: Twenty-Second Workshop on Geothermal Reservoir Engineering, Stanford University, Stanford, California.